Rare Metal Materials and Engineering
Volume 49, Issue 4, April 2020
Available online at www.rmme.ac.cn

Science Press

Cite this article as: Rare Metal Materials and Engineering, 2020, 49(4): 1191-1199.

ARTICLE

Microstructure and Space Tribological Properties of Laser Cladding NiCr-Ag Composite Coating on Pure Ti Substrate

Guo Chun, Chen Feng, Wei Baoli, Zhang Hua

Anhui Science and Technology University, Bengbu 233000, China

Abstract: The composite coating NiCr-Ag was successfully prepared on the pure Ti substrate by laser cladding to improve the space tribological properties of pure Ti, with hard phase NiCr as the reinforcing agent and Ag as the primary lubricating fillers. The composition and microstructure of the fabricated composite coating were investigated by X-ray diffraction (XRD), scanning electron microscopy-energy dispersive spectrometry (SEM-EDS), and high-resolution transmission electron microscopy (HRTEM). Furthermore, the space tribological properties were evaluated by the space tribological test system with a ball-on-disc tribometer against AISI-52100 ball counterpart under simulated space environment including atomic oxygen (AO), ultraviolet irradiation (UV), and high vacuum (VC), in comparison with atmospheric environment (AR). The results show that the composite coating has better tribological properties in atmospheric environment than in simulation space environment. Vacuum (without any moisture or hydrocarbons) and intense radiation in the space environment will induce severe oxidation on the surface of the coating, which weakens the enhancement of the coating and deteriorates the lubrication effect. The wear mechanism is abrasive wear in the atmospheric environment. Adhesion wear and plastic deformation are the predominant wear mechanism in the space environment as peeling pits and transferred Ni, Cr, and Ti can be found on the worn surface and the surface of the counterpart, respectively.

Key words: space tribology; laser cladding; wear mechanism; microstructure; laser in-situ reaction

In recent decades, with the rapid development of space science and manned space flight, especially the development of large space stations, the demand for various space equipment which has characteristics of slow running speed, large size, compact structure and high reliability becomes more and more urgent. The typical large-scale space activities include solar energy windsurfing system, optical earth observation system, large optical observation system, and two-dimensional pointing system, whose operating area is low earth orbit (LEO) with distance from the ground of 200~1000 km[1-3]. LEO space environment is very complex and harsh, where the large space activity system will be affected by various environmental factors such as high vacuum, ultraviolet radiation, atomic oxygen corrosion, thermal cycling and microgravity when the aerospace equipment runs at LEO[4,5]. Whether these space machines can operate normally and achieve their desired life depends on the friction and wear properties of the mechanical components in the spacecraft. Moreover, NASA studies show that a considerable proportion of failures of space mechanical motion components are associated with space lubrication. With the rapid development of aerospace technology, the general requirements for space mechanical tribology system can be summarized as low friction wear, low friction noise and long life. Thus, the tribological properties of the spatial mechanical friction pairs will inevitably exert a significant influence on the implementation of the entire space program, and have become the research focus in the field of international space friction materials and technology[6-8].

Titanium alloys have been used in a wide range of applications in aerospace, chemical, food, automotive, biomedical, and medical industries due to their high strength-to-weight ratio, excellent corrosion resistance, low density, high strength at elevated temperatures, and biological compatibility[9-11]. The demand for titanium alloys in the aerospace industry has steadily increased in consideration of

---

Received date: April 15, 2019

Corresponding author: Guo Chun, Ph. D., Associate Professor, College of Mechanical Engineering, Anhui Science and Technology University, Bengbu 233000, P. R. China, Tel: 0086-550-6734840, E-mail: guochun@ahstu.edu.cn

the above advantages of titanium alloys. Still unaddressed, however, the problem of poor tribological properties of titanium alloy restricts its working conditions and service life, especially in the environment of vacuum, which has been verified by previous experiments and practice applications[12]. Ti and Ti-alloy exhibit low surface hardness, poor wear resistance and higher friction coefficient under vacuum condition[13]. Yetim[14] proved that the friction coefficient of CP-Ti in the vacuum environment is not only very high but also extremely unstable due to the absence of lubricating film and moisture which can reduce the possibility of micro-welding occurrence on the worn surface. Besides, other researchers found that friction velocity and load have an important effect on the vacuum tribological properties of titanium alloy and cause changes in structural and phase, which may cause severe deformation and adhesion wear. Therefore, it is essential to use a surface treatment technology to improve the vacuum tribological properties of titanium alloys[15].

Laser cladding is an advanced surface modification technology with advantages of high energy density, fast cooling rate (10^5~10^6 °C/s), high processing speed with low dilution rate, fine solidification microstructure, and light segregation. What's more, the dense coating prepared by laser cladding contributes to reduce the diffusion of atomic oxygen in LEO environment. Laser cladding can achieve precise machining in micro scale with pretty heat affected zone and little thermal deformation, which is very suitable for processing precision parts operated in spacecraft[16-18].

The main purpose of current work is to prepare NiCr-Ag protective composite coating on the surface of pure Ti substrate by laser cladding, in order to improve the space tribological properties of pure Ti. The tribological properties of coatings in different space environments were systematically investigated, including atmospheric environment (AR), atomic oxygen (AO), ultraviolet irradiation (UV), and vacuum (VC). Furthermore, it is expected that the research result of the present work can provide technical and theoretical support for the engineering application of laser cladding nickel based alloy in aerospace industrial.

1 Experiment

1.1 Materials

Commercial pure Ti (TA2) (Fe<0.30 wt%, C<0.10 wt%, N<0.05 wt%, O<0.25 wt%, balance Ti) was machined into cylindrical specimens by wire-electronic discharging (31 mm in diameter, 10 mm in thickness) and used as substrate. Before laser cladding, pure Ti surface was washed with acetone, and sandblasted to further clean the working surface and got a rough surface to increase the surface absorption of laser. The principal raw material of the composite coating NiCr-Ag was 80 wt% NiCr (grit size 26~100 μm, purity>99%), and 20 wt% Ag (grit size 1.0~5.0 μm, purity 99.5%), and all the raw materials were in the form of powders. A high energy ball mill equipment (Fritsch Pulverisette P-4, made in Germany) was employed to make sure that all the powders were dispersed uniformly, with a rotary speed of 400 r/min for 10 h and the ball-to-powder mass ratio was fixed at 5:1. A mold whose inner diameter was 32 mm and interior can go up and down was used to pre-place powders. The substrate material (TA2) was placed in the middle of the mold. The height of the substrate was adjusted so a 1 mm deep groove formed between the substrate surface and the upper edge of the mold. The powders were prepositioned in the grooves, and compacted with a polished, smooth copper plate, thus forming a "puff cake" with 1 mm thickness at the grooves. The as-milled feedstock powders with a thickness of approximately 1 mm were pre-placed on the pure Ti substrate before laser cladding.

1.2 Preparation and characterization of composite coatings

The preparation of the composite coating was carried out by a 10 kW transverse flow continuous wave CO_2 laser processing system (DL-HL-10000B, China), which was connected to a computer for numerical controlling. The laser process parameters are as follows: the power of the laser beam was 2 kW, which was sufficient enough to get complete coatings; beam diameter was 3 mm with a focal length of 88 mm; the speed of traverse beam was 800 mm/min with overlapped tracks of 50%. Semi-open argon protection device with a pressure of 0.2 MPa was used as protective gas for preventing the coating from oxidation.

The as-obtained composite coatings were cooled to room temperature in the open air. Samples for tribological test (Φ24 mm×8 mm) and cross-sectional samples for structure characterization were prepared by wire cutting technology. The as-obtained samples were polished with SiC abrasive sandpaper (80#, 120#, 400#, 600#, 800#, 1000#, 1500# and 2000#) and then polished with 1.0 μm Al_2O_3 paste to eliminate surface scratches. Samples used for structural and compositional characterization require further processing in Koll's metallographic etching solution (4 vol%HF+2 vol%HNO_3+94 vol%H_2O) at room temperature for more than 4 min. The component and crystal structure of composite coating were characterized by a Philips D/max 2400 X-ray diffractometer (XRD, 40 kV, 100 mA, Cu-Kα radiation, 2θ=20°~70°). The observation of the microstructure of the cross-section of composite coating was performed by SEM-EDS (JEOL JSM-5600LV, Japan). A Tecnai-G2-F30 transmission electron microscope (TEM) operated at 300 kV was used to obtain HRTEM images. The micro-hardness profile along the depth direction of the composite coating (load: 1.96 N; dwell time: 5 s) was determined by a MH-5 Vickers micro-hardness tester.

1.3 Evaluation of space tribological properties of the composite coatings

The space tribological properties of the composite coating under ground simulated low earth orbit space environment were investigated by the ground simulated space tribology test system developed by Lanzhou Institute of Chemical Physics, Chinese Academy of Sciences. The tribological properties of pure Ti under four environmental conditions were tested: atmospheric environment (AR), atomic oxygen (AO), ultraviolet irradiation (UV), and vacuum (VC). The atmospheric environment conditions were relative humidity 45% and temperature 25 °C. All ground simulated LEO space environment experiments were carried out under a vacuum of 10^{-4} Pa. Individually, atomic oxygen irradiation experiments were conducted in a ground-based AO simulation system with impingement kinetic energy of 5.5 eV, and the average flux atomic oxygen density was 5×10^{15} atom/(cm^2·s), identical with the direct impact energy of AO to material surfaces that happened in LEO[19,20], and the samples were irradiated for 240 min. UV irradiance was conducted under ultraviolet irradiation conditions: the pressure in the test chamber was high vacuum, about 10^{-4} Pa, and the UV wavelength range was 115~400 nm. A typical UV energy flux at the sample position was determined to be 6 suns with an impingement kinetic energy of 5.5 eV, and the exposure period was controlled for 240 min, equivalent to 24 sun hours[21]. The space tribological properties of the composite coating were directly determined by a space tribological test system with ball-on-disc tester after atomic oxygen and ultraviolet radiation. Commercially available AISI52100 steel balls with a diameter of 3.175 mm and a hardness of 7000 MPa were used as the counterpart. The running-in process occurred under a load of 5 N with the diameter of rotation of 12 mm and a liner velocity of 0.1884 m/s. The friction coefficient was recorded automatically by a computer that was connected to the test rig and a dual-mode three-dimensional (3D) surface profiler (AEP, USA) was used to calculate the wear volume. The wear rate is calculated by Eq.(1)

$$K=V/F_n d \tag{1}$$

where V is wear volume (mm^3), F_n is load (N), d is friction distance (m), and W is wear rate (mm^3/(N·m))[22]. In order to ensure the reproducibility of the measurements and the accuracy of the results, each friction test was repeated at least three times under the same conditions. The morphology of the worn surfaces and the wear scar of the counterpart were analyzed by SEM. Moreover, EDS, which was connected to SEM, was used to analyze the element distribution of the counterpart AISI52100 steel balls.

2 Results and Discussion

2.1 Composition and microstructure of as-prepared composite coatings

Fig.1 shows the XRD pattern of the laser-processed composite coating. It can be seen that the main component of the composite coating is Cr_3Ni_2 and NiTi. Besides, Cr_2Ti, $TiCrN_2$, Cr_2Ti, TiAg and Ag can also be found in the composite coating with high contents. The original NiCr materials no longer exist and they are replaced by a series of intermetallic compounds produced by laser in-situ reactions. What's more, intense diffusion of material occurs between the coating and the substrate due to the high energy of the laser beam, and a large amount of Ti diffuses into the coating to in-situ react with the Ni, Cr and Ag in the composite coating, resulting in the formation of intermetallic compounds, such as NiTi, Cr_2Ti, $TiCrN_2$, Cr_2Ti and TiAg. Much more attention must be paid to $TiCrN_2$. A large amount of gas nitrogen permeates into the molten pool during the laser cladding process, and $TiCrN_2$ is generated by chemical reaction among Ti, Cr and N_2 in the molten pool. In addition to TiAg, there is a large amount of Ag which improves the tribological properties of the coating at room temperature.

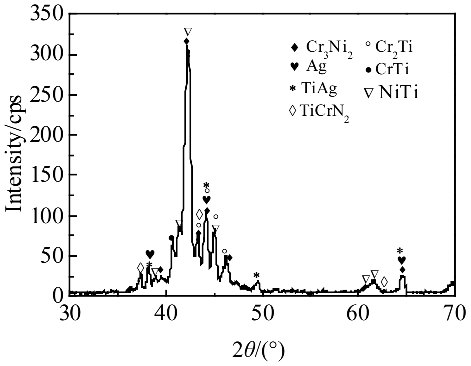

Fig.1 XRD pattern of the laser-processed composite coating

Fig.2a is the cross-sectional SEM image of the composite coating. A dense composite coating is obtained by laser cladding, which is finely metallurgically bonded with the substrate with nonporous and non-cracks coatings. The thickness of the composite coating is about 1.0 mm, and the bond line between the coating and the substrate is distinct while the appearance of white circular Ag particles is obvious. Element distribution of coating is characterized, as shown in Fig.2b~2e, Ni and Cr are uniformly distributed throughout the coating, indicating that most of them exist in the form of intermetallic compounds. It can be identified in Fig.2d that a part of Ag is dispersed in the whole coating and diffused into the substrate during laser cladding, while the remaining Ag is aggregated in the coating, which is marked as Ag particles in Fig.2a. The element mapping result coincides with the XRD result that there is only intermetallic compounds TiAg contain Ag except simple substance Ag. It is really dramatic that multitudinous Ag diffuses into the substrate during laser cladding[23].

Fig.3a shows the cross-sectional magnified SEM micrographs of near-top composite coating. The sub-cooling degree is large enough to nucleate the intermetallic compound in the molten pool simultaneously over a wide range, resulting in the formation of tiny nanoparticles (the size is less than 860 nm) with high nucleation rate. What's more, because the cooling

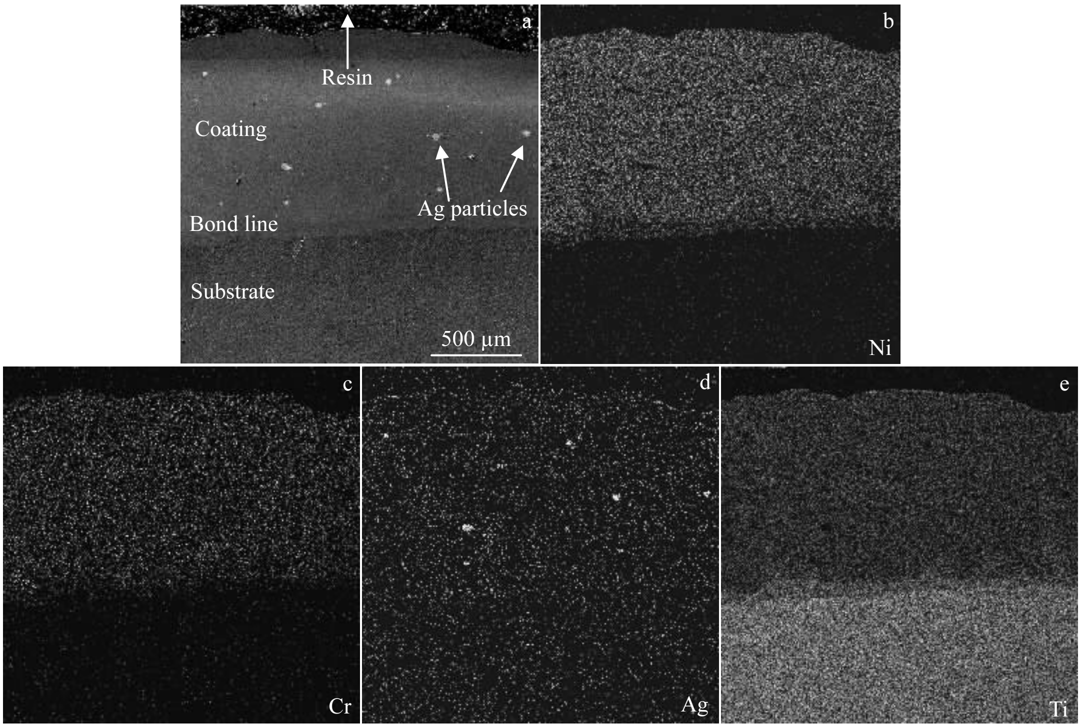

Fig.2 Cross-sectional SEM image (a) and EDS element mappings (b~e) of the composite coating

rate during melt quenching reaches 10^6 K/s, it will inhibit the formation and growth of larger crystals[24]. Nanoparticles are dense and uniformly distributed in regions close to the surface of the coating, while nanoparticles are randomly distributed in regions far from the surface. The temperature gradient increases gradually with decreasing the sub-cooling sharply as the distance to the substrate decreases. As a result, the crystallization rate slows down and large columnar crystals appear. It is also noticed that a large number of secondary crystals are formed around columnar crystals, forming a series of dendritic crystals. The interface of the composite coating is shown in Fig.3b. Neither nanoparticles nor columnar crystals and dendritic crystals appear. They are all replaced by cellular crystals with larger size. This is because the closer the position to the interface, the lower the cooling rate of the molten pool, and the grain can get enough growth time to become cellular crystals with greater grain size. Without that it can be observed that the metallurgical bonding zone between the cladding layer and the matrix is flat and clear, showing that the crystalline structure of "white band" forms under the condition of quench cooling.

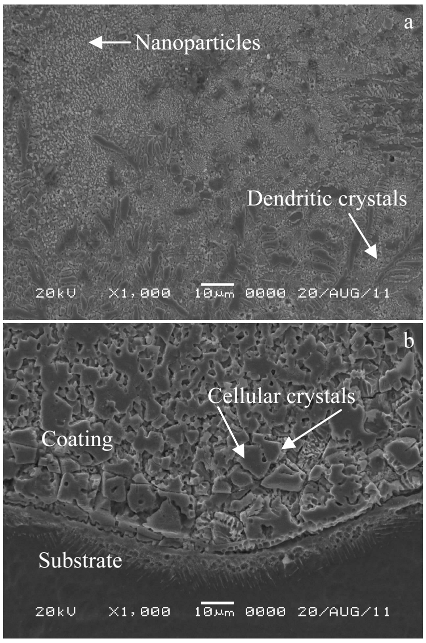

Fig.3 Cross-sectional magnified SEM images of composite coating: (a) top of the coating and (b) interface of the coating

In order to study the composition and microstructure of coatings in more detail, transmission electron microscopy (TEM) was used to character the laser cladding composite coating. The bright-field image in Fig.4a indicates that the composite coating consists of bright primary phase (area A) and black spherical nanoparticles (area B) with a size around 50 nm, which are randomly distributed throughout the coating. Subsequently, the corresponding selected area electron diffraction (SAED) results in Fig.4b show that the bright primary phases are intermetallic compounds NiTi, which are formed by laser in-situ reaction with crystal plane (300), (100), and $(2\bar{1}0)$. Furthermore, in Fig.4c, high resolution transmission electron microscopy (HRTEM) image of area B shows that its interplanar spacing is approximately 0.236 nm, which is accordant with interplanar spacing of Ag (111) plane. What's more, the size of Ag is nanometer scale, approximately 50 nm. The formation of these nanoparticles depends on the characteristics of rapid cooling specific to laser cladding. In comparison, it can be found that the compounds represented by TEM appear in the XRD results.

2.2 Microhardness

Fig.5 shows microhardness distribution on the cross-section of the laser cladding composite coating. The average microhardness of the coating is probably 8600 MPa which is 4.5 times larger than that of the substrate (the microhardness of Ti is about 1900 MPa). Although the microhardness of the coating varies slightly, the microhardness of the coating in the range of 400~850 μm is higher than near the surface. The hard reinforcement phases Cr_2Ti, $TiCrN_2$ and Cr_2Ti generated by laser in-situ reaction are the main reasons for the great increase of coating hardness. The regular structure induced by the quenching action of laser cladding as well as fine grain strengthening effect of nanoparticles will also improve the microhardness of the coating. The thermal convection in the molten pool during laser cladding is not sufficient to achieve complete dispersion of the hard particles. Compared with Ag which has a larger thermal expansion coefficient, the hard phase with smaller thermal expansion coefficient has a tendency to sink into the bottom of the molten pool during the process of solidification, so the hardness near the interface is relatively high. Moreover, although the microhardness of the coating decreases drastically at the interface, the microhardness of the interface near the coating side is still higher than that of the substrate. On the one hand, some Ti diffuses into the molten pool of the coating in the process of laser cladding, resulting in a sharp decrease in hardness of the coating[17]. On the other hand, it is possible that the surface of the substrate is annealed by the pre-melting of the powders during the cladding process, and the β-phase transformation occurs in the heat affected zone of the substrate by laser quenching. So the microhardness of the interface near the coating is higher.

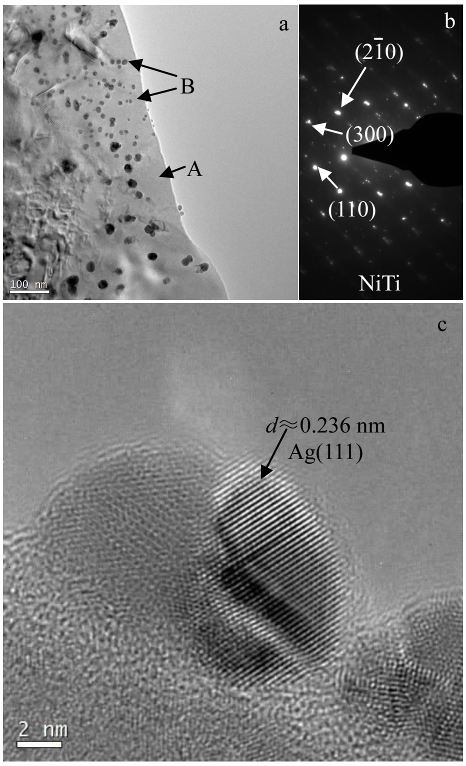

Fig.4 TEM bright field image of laser cladding composite coating (a); SAED pattern of area A in Fig.4a (b), and HRTEM image of area B in Fig.4a (c)

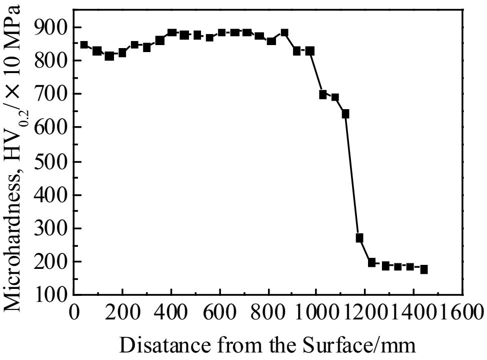

Fig.5 Microhardness distribution on the cross-section of the laser cladding composite coating

2.3 Space tribological properties of the laser cladding composite coating

Fig.6a is friction coefficient of the composite coating in the environment of atmospheric environment (AR), atomic oxygen (AO), ultraviolet irradiation (UV), and vacuum (VC). The composite coating has the smallest friction coefficient in the atmospheric environment, with a value of 0.408, and friction coefficient in the atomic oxygen is 0.530 which is the largest one among all the tests. Besides, in ground simulated space environment, the friction coefficients under ultraviolet irradiation (UV) and vacuum (VC) are 0.482 and 0.515, respectively. The results of our previous research show that the friction coefficients of TA2 substrate in atmospheric environment (AR), atomic oxygen (AO), ultraviolet irradiation (UV), and vacuum (VC) are 0.44, 0.67, 0.69 and 0.69, respectively[25]. Obviously, the friction coefficient of the coating prepared by laser cladding is much smaller than that of the substrate under the same test condition. The lubricity of the coating is greatly improved compared to that of the substrate.

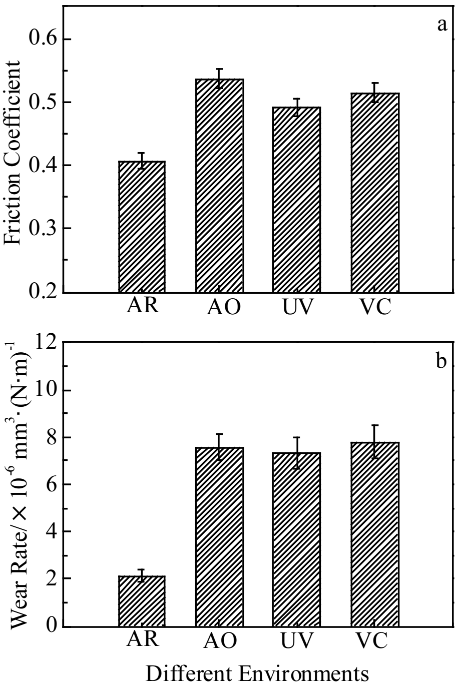

Fig.6 Friction coefficient (a) and wear rate (b) of the composite coating in different environments

But the friction coefficient of the coating under atomic oxygen, ultraviolet irradiation and vacuum conditions is much larger than in atmospheric environment. Equally, the wear rate of coatings shows the same variation trend. As shown in Fig.6b, the wear rate under atmospheric environment is the minimum one among all the research conditions, about 2.14×10^{-6} $mm^3/(N\cdot m)$, while the wear rates in the environment of AO, UV and VC are 7.65×10^{-6}, 7.39×10^{-6} and 7.82×10^{-6} $mm^3/(N\cdot m)$, respectively. Although the wear rate in the ground simulated space environment is much larger than in the atmospheric environment, it is at least 20 times lower than the tribological performance of the titanium alloy (TA2) substrate in the ground simulated space environment (the wear rate of the TA2 alloy in ground simulated space environment has been characterized under the same test conditions in previous work[25]). The reasons for this phenomenon can be explained as follows: Ag is a low temperature solid lubricating material which can play a lubrication role at atmospheric environment[26-28]. For good measure, small molecules such as H_2O adhered to the surface of a coating, together with other surface contaminants like hydrocarbons or hydrophilic oxides, play a role of lubricating medium and bring about "hydro-lubrication", resulting in a smaller friction coefficient[29]. But in the vacuum conditions, there are no small molecular substances such as H_2O or hydrocarbons. Strictly speaking, the worn surface is absolutely clean without lubricating medium on worn surface. In this case, hydro-lubrication does not occur and the friction coefficient becomes larger. So the coating exhibits low friction coefficient and good wear resistance in AR. Three kinds of ground simulated spatial friction test conditions have the same degree of vacuum, so we can conclude that the vacuum in the space environment has a great influence on the space tribological properties of the coating. It is generally known that AO has high activity with the collision kinetic energy of 5.0 eV in the ground simulated space environment, which is equivalent to thousands of degrees Celsius. So the composite coating is subjected to severe oxidation and erosion caused by high temperature oxidation and high speed collisions of AO[30]. As a result, Ag will be oxidized and replaced by AgO or Ag_2O without lubrication effects. The composite coating loses lubrication and the friction coefficient increases[31, 32]. Otherwise, in space environment (such as AO and UV), the oxide film on the coating surface is removed rapidly during the friction process, and the regeneration is so difficult that the surface of the friction pair is in exposed state with fresh surface contact. What's even worse, it is prone to "sticky" or even "cold welding" between clean surface with the increase of adhesion and shearing force, making the friction pair unable to move relatively[33]. While in the vacuum environment (VC) which is a completely clean environment, there is no moisture and other small molecules which may cause "hydro-lubrication" failure. As a result, the space tribological properties of the coating in the space environment (including AO, UV and VC) decrease palpably.

Wear morphologies of the composite coating in different environments were characterized by SEM, as shown in Fig.7. Fig.7a shows the worn surface in atmospheric environment. The image reveals that a great number of wear debris appears on the worn surface, resulting in irregular worn surface. The emergence of grooves cannot be found, indicating that there is no three-body wear caused by wear debris. This further confirms that the coating has a lower wear rate in atmospheric environment. According to the conjecture, the perfect mechanical properties (such as high microhardness) of the coating are one of the main reasons for the avoidance of three body wear. Meanwhile, the lubrication effect of Ag is also conducive to reduce the damage of wear debris on worn surface. It illustrates that the predominant wear mechanism is abrasive wear.

Fig.7b and 7c are the images of the worn surface under atomic oxygen (AO) and ultraviolet irradiation (UV), it can be seen that the worn surface morphologies of both coatings are similar. It is speculated that the fierce oxidation of atomic oxygen (AO) and the effect of ultraviolet radiation (UV) lead to serious oxidation of worn surface, resulting in intermittent oxide film whose main components are NiO, TiO_2, Cr_2O_3, AgO and Ag_2O. Quite apart from that, a large number of peeling pits due to adhesive wear are found in the coating. Oxidation of the coating in harsh space environment gives rise to such phenomenon. On the one side, the oxidation rate depends on whether the coating still has a protective effect as AO is transported through the oxide layer via diffusion-mechanism and gas-flow process. The internal stress will appear between the oxide layers because of the mismatch in ratio between sliver oxide (including AgO and Ag_2O) and Ag, which induces serious peeling pits and deformation of oxide layer. Furthermore, the source of the internal stress is not only one, internal stress caused by oxidation itself may also further exacerbate deformation and peeling pits[34]. The decline in mechanical properties (such as hardness) also brings severe plastic deformation, and the surface of the coating is easy to be abraded as the coating is oxidized. On the other side, the wettability between the oxidized coating and the substrate deteriorates and the bonding strength becomes weak, resulting in a greater wear on the wear surface. During the wear process, the wear debris will adhered to dual surface instead of throwing away the worn surface, increasing the wear rate and also leaving peeling pits on the worn surface. It indicates that adhesion wear and plastic deformation are the main wear mechanism.

The worn surface of the coating under vacuum (VC) environment is shown in Fig.7d. The peeling pit on the worn surface is larger than that in the environment of AO and UV. Compared with metal oxides, metal elements and metal alloys have better wettability with counterpart. As a result, much more debris will stick to the counterpart, giving rise to enormous peeling pits on the worn surface. This agrees with the change of wear rate of the composite coating under different environments. Adhesive wear is the primary wear mechanism.

Fig.8 is the worn morphologies of counterpart AISI52100 steel balls and corresponding map distribution of Fe, Ni, Cr and Ti under different environments. There are a handful of Ni, Cr, and Ti elements on the counterpart surface, so it is believed that there is no significant element transfer on the counterpart in atmospheric environment (AR), indicating that scarcely no adhesive wear occurs. Except atmospheric environment, the three elements (Ni, Cr and Ti) also undergo obvious transfer in other ground simulated space environments (such as AO, UV, and VC). Moreover, the Fe element does not appear on the counterpart wear mark when tested under ground simulated space environment as the transfer films on the counterpart are thick enough to shield Fe. Simultaneously, the surface element distribution of counterpart in three kinds of friction test environments (AO, UV, and VC) is compared. It can be seen that the content of Ni, Cr and Ti in the surface of the counterpart when it is in vacuum environment is much higher than in environment of atomic oxygen (AO) and ultraviolet irradiation (UV). This shows that when there is only a vacuum environment without atomic oxygen or ultraviolet radiation, the adhesion between the coating and the counterpart is enhanced during the wear process, and these results coincide with the result shown in Fig.7.

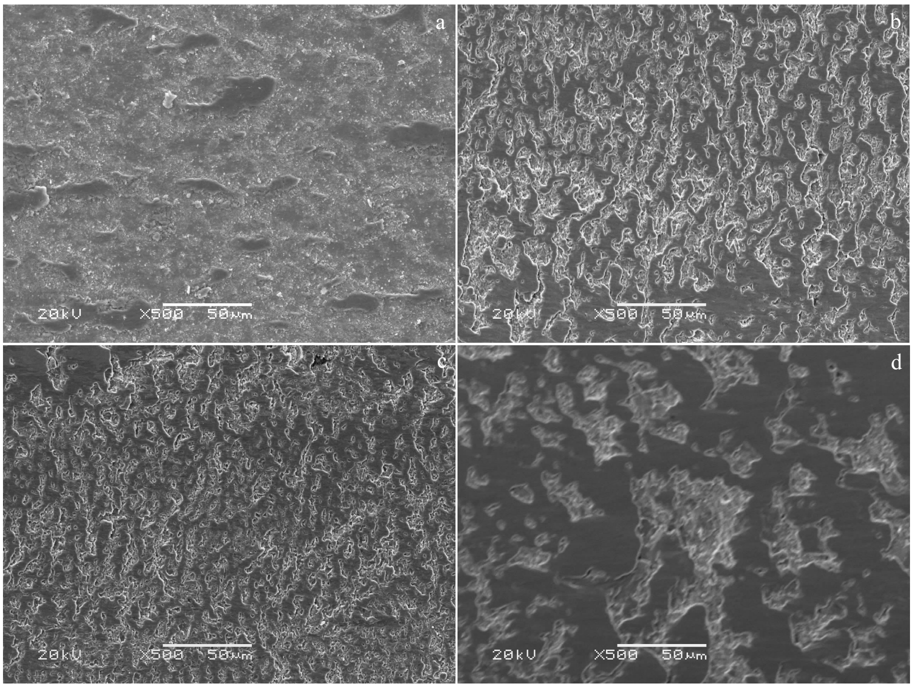

Fig.7 Wear morphologies of composite coatings in different environments: (a) atmospheric environment (AR), (b) atomic oxygen (AO), (c) ultraviolet irradiation (UV), and (d) vacuum (VC)

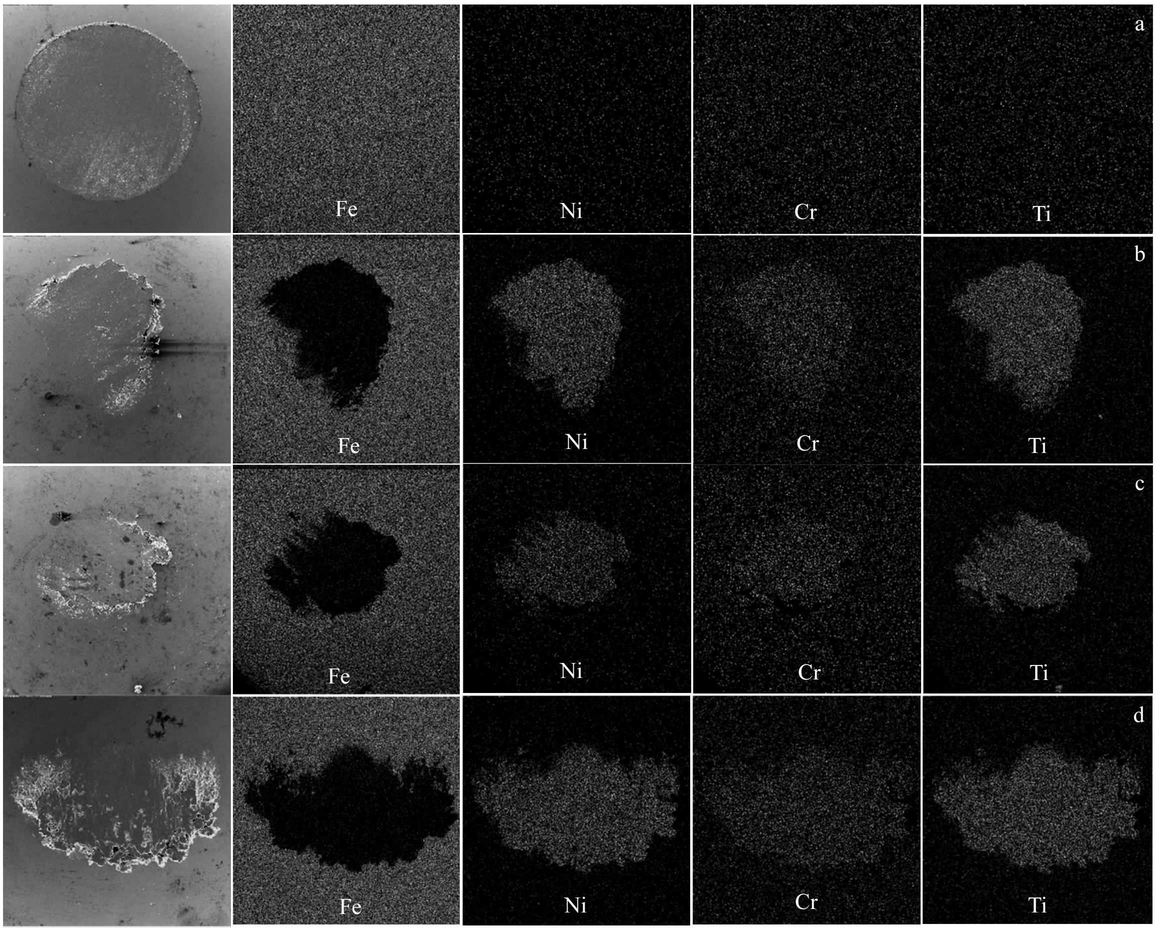

Fig.8 Worn morphologies of counterpart AISI52100 steel balls and corresponding map distribution of Fe, Ni, Cr and Ti under environment of AR (a), AO (b), UV (c), and VC (d)

3 Conclusions

1) A compact NiCr-Ag composite coating which has good metallurgical bond with the substrate without pores and cracks is prepared by laser cladding. In addition to primary component Ag, the composite coating also consists of Cr_3Ni_2, NiTi, Cr_2Ti, $TiCrN_2$, Cr_2Ti, and TiAg, which are formed by laser in-situ reaction between the coating and the Ti alloy substrate.

2) The average microhardness of the coating is approximately 8600 MPa which is 4.5 times larger than that of the substrate. A large number of hard reinforcement phases Cr_2Ti, $TiCrN_2$ and Cr_2Ti generated by laser in-situ reaction are homogeneously distributed and the regular structure induced by the quenching action of laser cladding as well as fine grain strengthening effect of nanoparticles bears the primary responsibility for improvement of microhardness.

3) The tribological properties of the composite coating under atmospheric environment are much better than in the ground simulated space environment (including atomic oxygen, ultraviolet irradiation, and vacuum), which suggests that the tribological properties of the coatings are very sensitive to the space environment. Moreover, the coating undergoes the most severe wear in the vacuum environment, due to the fact that the average wear (and friction) in high vacuum environment is actually higher. But the tribological performance of the composite coating in the ground simulated space environment is greatly improved compared with titanium alloy substrate.

4) The wear mechanism is abrasive wear under atmospheric environment, indicated by randomly distributed debris. Adhesion wear and plastic deformation are the main wear mechanism under ground simulated space environment (AO, UV, and VC) as peeling pits and transferred Ni, Cr, and Ti on the counterpart can be found on the worn surface and the surface of the counterpart, respectively.

References

1 Tagawa Masahito, Yokota Kumiko, Ochi Kunitaka *et al.* *Tribology Letters*[J], 2012, 45(2): 349

2 Gao Xiaoming, Fu Yanlong, Jiang Dong *et al.* *Tribology Letters*[J], 2018, 66(4): 137

3 Wang Xiaohan, Li Yixuan, Qian Yuhai *et al*. *Advanced Materials*[J], 2018, 30(36): 1 803 854

4 Duo Shuwang, Song Mimi, Liu Tingzhi *et al*. *Rare Metal Materials and Engineering*[J], 2011, 40(S1): 488

5 Kayhan Neda, Razavi Reza Shoja, Choopani Saeed. *Progress in Organic Coatings*[J], 2012, 74(3): 603

6 Gao Xiaoming, Fu Yanlong, Jiang Dong *et al*. *Surface & Coatings Technology*[J], 2018, 353: 8

7 Longhurst William R, Cox Chase D, Gibson Brian T *et al*. *International Journal of Advanced Manufacturing Technology*[J], 2017, 90(1-4): 81

8 Tagawa M, Yokota K, Matsumoto K *et al*. *Surface & Coatings Technology*[J], 2007, 202(4-7): 1003

9 Zhang Jinyong, Li Jinshan, Chen Zheng *et al*. *Rare Metal Materials and Engineering*[J], 2018, 47(9): 2787 (in Chinese)

10 Yang Xiaokang, Wang Kuaishe, Shi Jiamin *et al*. *Rare Metal Materials and Engineering*[J], 2018, 47(8): 2341

11 Veiga C, Devim J P, Loureiro A J R. *Reviews on Advanced Materials Science*[J], 2012, 32(2): 133

12 Hager C H, Sanders J H, Sharma S. *Wear*[J], 2006, 260(4-5): 493

13 She Dingshun, Yue Wen, Fu Zhiqiang *et al*. *Surface & Coatings Technology*[J], 2015, 264: 32

14 Yetim A F. *Surface & Coatings Technology*[J], 2010, 205(6): 1757

15 Straffelini G, Molinari A. *Wear*[J], 1999, 236(1-2): 328

16 Brueckner F, Lepski D, Beyer E. *Journal of Thermal Spray Technology*[J], 2007, 16(3): 355

17 Liu Xiubo, Meng Xiangjun, Liu Haiqing *et al*. *Materials & Design*[J], 2014, 55: 404

18 Li Zhengxue, Liu Hongxi, Zhang Xiaowei *et al*. *Rare Metal Materials and Engineering*[J], 2018, 47(5): 1437 (in Chinese)

19 Ji Li, Li Hongxuan, Zhao Fei *et al*. *Applied Surface Science*[J], 2009, 255(7): 4180

20 Gamulya G D, Ostrovskaya E L, Yukhno T P. *Powder Metallurgy and Metal Ceramics*[J], 2001, 40(3-4): 135

21 Wu Yanxia, Liu Ying, Yu Shengwang *et al*. *Tribology Letters*[J], 2016, 64(2): 24

22 Gilley Kevin L, Nino Juan C, Riddle Yancy W *et al*. *ACS Applied Materials & Interfaces*[J], 2012, 4(6): 3069

23 Baldridge T, Poling G, Foroozmehr E *et al*. *Optics and Lasers in Engineering*[J], 2013, 51(2): 180

24 Zhu Hongmei, Chen Minghui, Tang Zhongfeng *et al*. *Rare Metal Materials and Engineering*[J], 2019, 47(9): 2767 (in Chinese)

25 Guo Chun, Yao Rungang, Kong Hongyu *et al*. *Surface and Coatings Technology*[J], 2014, 246: 40

26 Aouadi S M, Singh D P, Stone D S *et al*. *Acta Materialia*[J], 2010, 58(16): 5326

27 Aouadi S M, Paudel Y, Simonson W J *et al*. *Surface & Coatings Technology*[J], 2009, 203(10-11): 1304

28 Aouadi Samir M, Paudel Yadab, Luster Brandon *et al*. *Tribology Letters*[J], 2008, 29(2): 95

29 Suszko T, Gulbinski W, Jagielski J. *Surface & Coatings Technology*[J], 2006, 200(22-23): 6288

30 Donnet C, Martin J M, Lemogne T *et al*. *Tribology International*[J], 1996, 29(2): 123

31 Zheludkevich M L, Gusakov A G, Voropaev A G *et al*. *Oxidation of Metals*[J], 2004, 61(1-2): 39

32 Li Long, Yang Judith C, Minton Timothy K. *Journal of Physical Chemistry C*[J], 2007, 111(18): 6763

33 Nishimura M. *JSME International Journal Series Iii-Vibration Control Engineering for Industry*[J], 1988, 31(4): 661

34 Xiong Y Q, Liu L M, Lu W G *et al*. *Materials Science and Engineering B-Solid State Materials for Advanced Technology*[J], 2001, 79(1): 68

钛表面激光熔覆 NiCr-Ag 复合涂层组织结构及空间摩擦学性能

郭　纯，陈　丰，魏宝丽，张　华

(安徽科技学院，安徽 蚌埠 233000)

摘　要：利用激光熔覆技术在钛基材表面制备了 NiCr-Ag 复合涂层。用 XRD、SEM 和 HRTEM 分析了涂层的组成和组织结构，利用空间摩擦学系统对复合涂层在 3 种模拟空间环境（高真空、原子氧和紫外辐照）以及大气环境下的摩擦磨损性能进行了研究。采用 SEM 和 EDS 对磨损后复合涂层和对偶钢球的形貌和元素面分布进行了分析，揭示了复合涂层在模拟空间环境及大气环境下摩擦磨损失效机理。结果表明：复合涂层在大气环境条件下的摩擦磨损性能优于在 3 种模拟空间环境下的摩擦磨损性能；真空下的辐照对复合涂层的摩擦磨损性能有显著的影响，辐照会增加涂层表面氧化；复合涂层在高真空、原子氧和紫外辐照模拟空间环境下的磨损机理为较严重的粘着磨损、磨粒磨损和塑性变形，在大气环境条件下的磨损机理主要为磨粒磨损。

关键词：空间摩擦；激光熔覆；磨损机理；结构；激光原位反应

作者简介：郭　纯，男，1984 年生，博士，副教授，安徽科技学院机械工程学院，安徽 蚌埠 233000，电话：0550-6734840，E-mail: guochun@ahstu.edu.cn